

ANAMOLOUS MORPHOLOGICAL SCALING IN EPITAXIAL NIOBIUM THIN FILMS ON MGO(001)*

D. Beringer[#], W. M. Roach, C. Clavero and R. A. Lukaszew, The College of William and Mary, Williamsburg, VA 23187, U.S.A.

C. E. Reece, Thomas Jefferson National Accelerator Facility, Newport News, VA 23606, U.S.A.

Abstract

Surface and interface roughness are critical factors in determining the properties and technological viability of many systems. These considerations are of principle importance for the development of next-generation superconducting radio frequency (SRF) cavities where the ultimate surface determines the cavity performance. The predominant SRF technology currently used in linear accelerators is based on bulk niobium cavities, however on-going efforts to improve cavity performance have considered the possibility of multi-layered thin film coatings on SRF cavities. In particular, Superconducting / Insulating / Superconducting (SIS) multilayer structures have been proposed as a means to achieve higher field gradients in SRF cavities and overcome fundamental SRF limitations of bulk niobium [1].

Nucleation and growth kinetics influence epitaxial thin film growth on different substrates. In addition, film properties differ from those in bulk systems mainly because of limited material supply as well as stress contributions due to lattice mismatch, which can induce significant surface roughness. Rough surfaces may lead to undesirable effects for SRF applications, many of which can be minimized with suitable choices of thin film growth parameters.

We have undertaken a systematic effort to understand the dynamic evolution of the Nb surface under specific deposition conditions. Here we examine the morphology of epitaxial Nb grown on MgO ceramic substrates at very low growth rates and closely examine the dynamical scaling of the surface features during growth.

DYNAMICAL SCALING

Family-Vicsek Scaling

The Family-Vicsek scaling ansatz assumes that non-equilibrium processes take on a scale invariant form in both space and time and can be fully characterized by a finite set of scaling parameters. It is assumed that stochastic processes drive the surface evolution and that the resulting features will have a self-affine form. In this scenario, the dynamic evolution of the roughness of the system in question can be fully described by a pair of scaling exponents, α and β , the global roughness exponent

and growth exponent respectively. These experimentally determined parameters, when compared with ones calculated from growth models, will implicate particular, responsible growth mechanisms and serve to classify these processes within scaling universality classes [2].

Here it is assumed that the correlation functions will assume a power-law form and that the Family-Vicsek dynamic scaling ansatz

$$w(L, t) = t^\beta f(L/\xi(t))$$

will hold. The function $f(u)$ takes the form

$$f(u) \sim \begin{cases} u^\alpha & \text{if } u \ll 1 \\ \text{constant} & \text{if } u \gg 1 \end{cases}$$

The surface interface width $w(L, t)$, taken essentially to be the RMS roughness of the surface averaged over the lateral length L after certain time t (or equivalently film thickness), has two distinct asymptotic regimes depending on the length scale examined: $w(L, t) \sim L^\alpha$ for $L \ll L_c$ and $w(L, t) \sim t^\beta$ when $L \gg L_c$. Here, L_c (nominally taken to be morphological island size) defines a critical length scale over which the surface features are no longer correlated and scales as $t^{1/z}$, where $z = \alpha/\beta$ is the dynamic exponent.

General Dynamical Scaling

The self-affine approach to dynamical scaling has been successfully applied to a vast array of dynamic surfaces (such as the erosion of coastlines, chemical etching processes, ballistic deposition, etc.); however, there are certain systems in which the scaling patterns demonstrate aberrant behaviour between the global (long range or saturated) and local (short) length scales. In this case, a common set of scaling exponents is no longer adequate to simultaneously characterize the disparate global and local dynamic scaling behavior; hence, additional local scaling parameters are necessary to fully classify surfaces that demonstrate this so-called *anomalous* scaling.

General Dynamical Scaling applies a more generic, yet analogous, scaling ansatz, formulated in Fourier space, which introduces an additional independent scaling parameter that can be used to classify anomalous scaling into invariant subclasses [3]. Here the ansatz is that the Power Spectral Density (PSD) defines a structure factor S

$$S(\mathbf{k}, t) = \langle H(\mathbf{k}, t)H(-\mathbf{k}, t) \rangle$$

*Work supported by

Department of Energy: DE-AC05-06OR23177

Defense Threat Reduction Agency: HDTRA1-10-1-0072.

[#]dbberinger@email.wm.edu

where H is the Fourier transform of the surface height function, k is the spatial frequency, and t the time (or film thickness). $S(k, t)$ assumes the general form (for a 2+1 dimensional system)

$$S(k, t) = k^{-(2\alpha_s+2)} t^{2(\alpha_{loc}-\alpha_s)/z}$$

and the spectral exponent α_s quantitatively captures the anomalous scaling independent of local and global values for α and β . The value of the spectral exponent, evaluated from the slope of the log-log plot S vs. k in the realm of large k , demarcates scaling behaviour by

$$\begin{cases} \alpha_s < 1 \Rightarrow \alpha_{loc} = \alpha_s \begin{cases} \alpha_s = \alpha \Rightarrow \text{Family-Vicsek} \\ \alpha_s \neq \alpha \Rightarrow \text{intrinsic} \end{cases} \\ \alpha_s > 1 \Rightarrow \alpha_{loc} = 1 \begin{cases} \alpha_s = \alpha \Rightarrow \text{super-rough} \\ \alpha_s \neq \alpha \Rightarrow \text{new class.} \end{cases} \end{cases}$$

Some recent studies have led to the hypothesis that large scaling exponents, i.e. $\alpha > 1$, and anomalous roughening of the growing surfaces are a consequence of non-local effects such as hindered diffusion and shadow instabilities [4]. Clearly a systematic study controlling parameters affecting the kinetics of the growth may clarify these mechanisms.

EXPERIMENTAL METHODS

Epitaxial Nb films were grown directly on MgO(001) substrates in an ultra-high vacuum (UHV) deposition system with a base pressure in the low 10^{-9} Torr range. Prior to deposition, each polished MgO substrate was ultrasonically cleaned in subsequent 10 minute baths of acetone and methanol. A pre-deposition annealing treatment for 1 hour at 600°C was carried out in order to degas and recrystallize the surface layers of each substrate. Nb films with thicknesses ranging from 10 to 600 nm were prepared under otherwise identical deposition conditions with a growth temperature of 600°C . The films were deposited using DC magnetron sputtering with an argon working gas pressure of 1.0 mTorr. The power delivered to the Nb target was 60 W. Growth rates for the thin films, as determined by X-ray reflectivity (XRR) and ellipsometry, were $0.32 \text{ \AA}/\text{sec}$.

Reflection high energy electron diffraction (RHEED) was employed to collect structural information *in situ* at various stages of Nb film growth in order to understand the relative crystallography of the Nb/MgO system. Characteristic RHEED patterns were collected for each MgO substrate along two distinct crystallographic directions corresponding to MgO[100] and MgO[110] azimuths.

Niobium is a strong getter and rapidly oxidizes with exposure to atmosphere; therefore, atomic force microscope (AFM) images were collected *ex situ* with a Nanotec instrument for each sample immediately upon removal from the UHV system in order to capture representative surface images [5]. Self-correlation as well

as statistical methods were applied to extract anisotropic lateral correlation lengths (average island size). The global and local surface interface widths were taken from RMS roughness data. PSD software was used to average spectral features of the thin films.

MORPHOLOGY AND STRUCTURAL CORRELATIONS IN Nb(110)/MgO(001)

RHEED images (Figure 1) taken along two distinct azimuthal directions in the Nb/MgO system indicate an epitaxial, mixed-phase Nb structure where Nb(110)/MgO(001) is present with two possible azimuthal crystalline orientations, namely Nb[110]||MgO[100] and Nb[110]||MgO[010]. The observation that Nb(110) achieves this particular registry with the underlying MgO(001) substrate is consistent with literature [6]. Each film throughout the thickness series shares these structural characteristics.

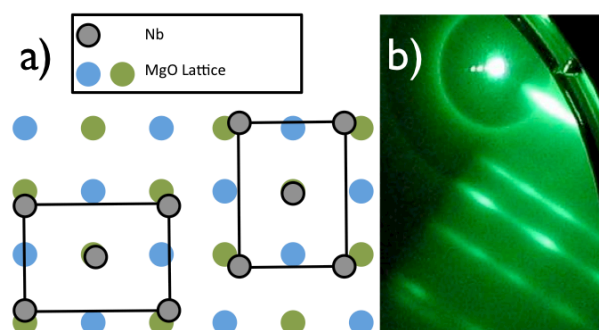


Figure 1: a) Atomic representation of the Nb(110)/MgO(001) epitaxy and b) RHEED image of the 100 nm Nb Film taken along MgO[001] azimuth.

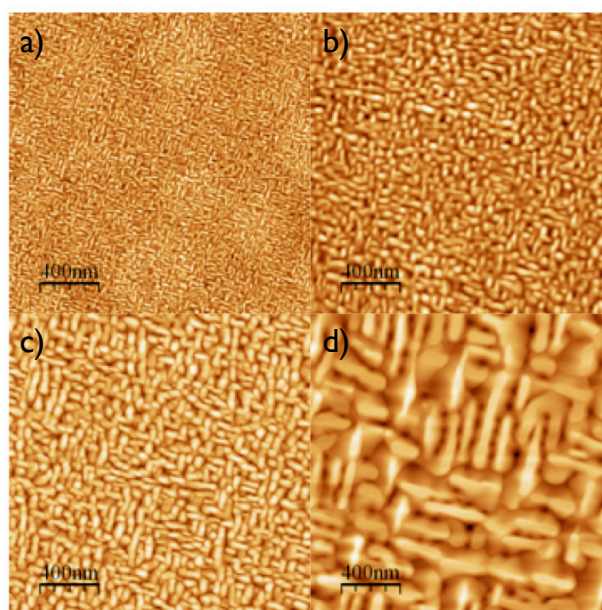


Figure 2: representative $2\mu\text{m} \times 2\mu\text{m}$ AFM scans for a) 30 b) 50 c) 100 and d) 600 nm Nb films. Note the similar morphological features throughout thickness series.

The horizontal direction in each AFM (Atomic Force Microscope) scan (Figure 2) was taken parallel to the MgO[001] direction. A clear biaxial morphological anisotropy is manifest and persistent throughout the thickness series. Suggestively, the direction and relative orientation of the morphological anisotropic features are consistent with structural anisotropies observed with RHEED.

GENERAL DYNAMIC SCALING IN NB(110)/MGO(001)

Global and Local Scaling Parameters

Global scaling parameters were extracted from the AFM scans over the thickness series. The auto-correlation of AFM images provides a means for identifying the average island size by fitting them to Gaussians and calculating their FWHM value. The nature of the observed anisotropy is biaxial; hence, the auto-correlation function, which was taken along the fast scan direction, is a convolution of the average island size along the major and minor anisotropy axes. Fitting a convolution of Gaussians allows for the determination of a global and anisotropic values for β/α . The values $(\beta/\alpha)_{width} = 0.4$ and $(\beta/\alpha)_{length} = 0.55$ as well as $\beta = 0.6$ were found from linear fits from the relevant log-log plots (see Figure 3). Anisotropic values for global α were calculated to be $\alpha_{length} = 1.1$ and $\alpha_{width} = 1.5$ with an average $\alpha_{avg} = 1.3$, which was derived from a radial average of the auto-correlation function.

Local scaling parameters were obtained via real space methods by analyzing line scans constrained along the tops of the morphological islands. The local values $\alpha_{loc} = 0.66$ and $\beta_{loc} = 0.34$ were obtained (see Figure 3). Here we see clear deviation between the local and calculated global scaling parameters indicating anomalous scaling.

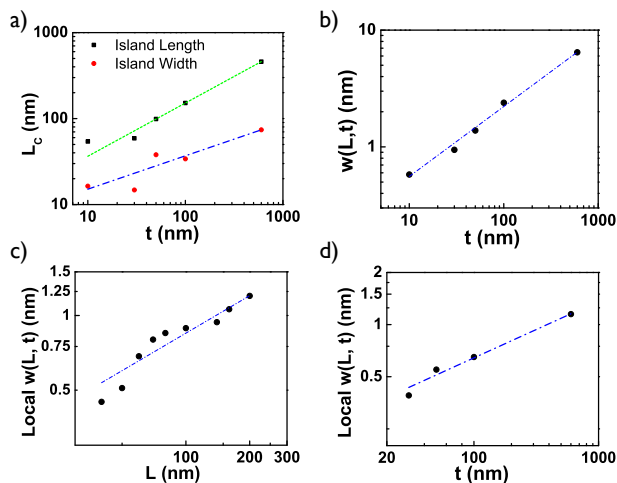


Figure 3: Logarithmic plots of a) island size (anisotropic) vs. film thickness b) global interface width vs. film

thickness c) local interface width vs. scan size and d) local interface width vs. film thickness.

Spectral Scaling Exponent

The spectral exponent was determined from the thickest film, $\alpha_s = 1.38$, and is close the global static coarsening exponent (Figure 4). The peak intensity from each curve is shifted to the left with increasing thickness, which corresponds to the more coarse periodic morphological features of the thin films. There also appears to be a vertical shift in the power spectrum with respect to increasing thickness as well. This suggests that $\alpha_s \neq \alpha_{loc}$ which is consistent with our results for the local scaling exponents.

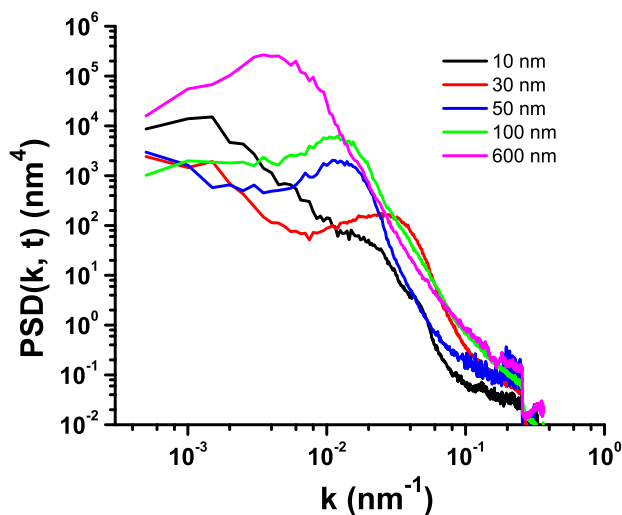


Figure 4: PSD curves for the Nb thickness series.

DISCUSSION

The scaling exponents suggest super-rough anomalous scaling in this Nb/MgO system for the particular set of deposition parameters explored. That $\alpha_{loc} < 1$ deviates from the theoretical value has been observed in other super-rough systems and has been attributed to intrinsic computational limits over these short length scales [4, 7].

REFERENCES

- [1] A. Gurevich, Appl. Phys. Lett. **88**, 012511 (2006).
- [2] F. Family and T. Vicsek, J. Phys. A **18**, L75 (1985).
- [3] J. J. Ramasco, J. M. Lopez and M. A. Rodriguez, Phys. Rev. Lett. **84**, 2199 (2000).
- [4] B. C. Mohanty, H. R. Choi, Y. S. Cho, EPL, **93**, 26003 (2011).
- [5] I. Horcas, R. Fernandez, J. M. Gomez-Rodriguez, J. Colchero, J. Gomez-Herrero and A. M. Baro, Rev. Sci. Instrum. **78**, 013705 (2007).
- [6] T. E. Hutchinson, J. Appl. Phys. **36**, 270 (1965).
- [7] M. A. Auger, L. Vazquez, R. Cuerno, M. Castro, M. Jergel and O. Sanchez, Phys. Rev. B, **73** 045436 (2006).